
Reducing Bias in Federated Class-Incremental Learning with Hierarchical Generative Prototypes

Riccardo Salami* **Pietro Buzzega*** **Matteo Mosconi** **Mattia Verasani** **Simone Calderara**

AIImageLab - University of Modena and Reggio Emilia, Modena, Italy
 name.surname@unimore.it

Abstract

Federated Learning (FL) aims at unburdening the training of deep models by distributing computation across multiple devices (clients) while safeguarding data privacy. On top of that, Federated Continual Learning (FCL) also accounts for data distribution evolving over time, mirroring the dynamic nature of real-world environments. In this work, we shed light on the *Incremental* and *Federated* biases that naturally emerge in FCL. While the former is a known problem in Continual Learning, stemming from the prioritization of recently introduced classes, the latter (*i.e.*, the bias towards local distributions) remains relatively unexplored. Our proposal constrains both biases in the last layer by efficiently fine-tuning a pre-trained backbone using learnable prompts, resulting in clients that produce less biased representations and more biased classifiers. Therefore, instead of solely relying on parameter aggregation, we also leverage generative prototypes to effectively balance the predictions of the global model. Our method improves on the current State Of The Art, providing an average increase of +7.9% in accuracy.

1 Introduction

The traditional paradigm in Deep Learning necessitates accessing large-scale datasets all at once, which hinders scalability and raises significant privacy concerns, especially when sensitive data is involved. Although distributing training across many devices could be an effective solution, there is still no effective mechanism for blending the resulting trained models into a single unified one. Federated Learning (FL) [34] addresses this challenge through a centralized server that coordinates distributed devices, aiming to create a single unified model while minimizing communication costs.

Federated Class-Incremental Learning (FCIL) [46, 9, 50] takes a step further and couples distributed training with Online Learning, tolerating distribution shifts in the data over time. This presents new challenges, as deep models learning online (without relying on old examples) experience severe performance degradation due to Catastrophic Forgetting [32]. In FCIL, the training process unfolds in tasks, each of which shifts the data distribution by introducing new categories. Each task is divided into communication rounds, wherein the local models train on their private data distribution. After local training, each client may transmit information to the orchestrator (server), which creates a global model and redistributes it to all clients. In the literature, some methodologies account for architectural heterogeneity (*i.e.*, heterogeneous FL [7, 18, 14]), while others aim to enhance the performance of local models without necessarily converging to a global one (*i.e.*, personalized FL [5, 31, 35]). Instead, we follow the original FCIL setting as presented in [9], with the goal of training a single global model in a distributed way.

*Equal contribution

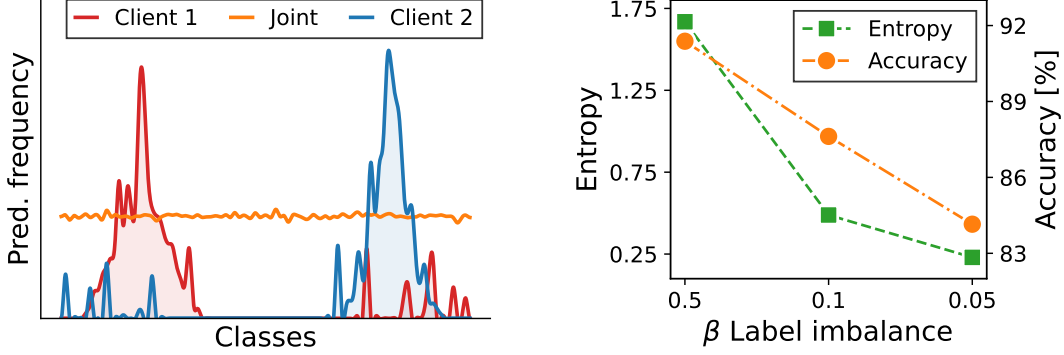


Figure 1: **Federated bias.** Histogram of the clients’ responses, computed on the global test set, for $\beta = 0.05$. Class indexes have been rearranged for improved visualization (left). The entropy of the response histograms, averaged on all clients, compared with FL performance (right).

When incrementally learning on a sequence of tasks, the model struggles the most at differentiating classes from distinct tasks, whereas it works well at separating those within the same one. Albeit one would intuitively link such behavior to catastrophic forgetting, it primarily occurs because tasks are learned in isolation, and some classes are never seen simultaneously [17]. This causes a bias towards recently introduced classes, which we refer to as *Incremental Bias* (IB). The authors of [30] observe a similar tendency in the Federated Learning scenario: since clients train exclusively on their local datasets, they exhibit a strong bias towards their local label distribution. We refer to this effect as *Federated Bias* (FB).

FB hits each client differently: following the local distribution trend, it drives the models’ responses in divergent directions. Consequently, its strength increases with the growing heterogeneity in the clients’ data distribution, suggesting a correlation with declining performance (see Section 2). To relieve such an effect, we constrain FB to the last layer by leveraging a frozen pre-trained backbone and efficiently fine-tuning it via prompt learning. Ideally, prompting keeps the clients’ representations close to the pre-training optimum (hence, close to each other), thus minimizing their Federated Bias. In Section 4.3, we experimentally verify that prompting leads to reduced bias in the feature space w.r.t. fine-tuning all parameters. Consequently, this confines the impact of FB to the last layer, providing the centralized server with less biased representations. On top of that, prompt-based methodologies *i*) have demonstrated SOTA results in Class-Incremental Learning [44, 43, 40] and *ii*) adapt only a small portion (less than 1%) of the clients’ parameters, enabling unmatched communication efficiency in distributed scenarios [51, 28] (see Appendix A for more details).

The authors of [45, 49, 30] address either IB or FB by fine-tuning the classification layer (where such biases are the most evident) on IID data samples. To meet the privacy requirements of FL, which prohibit transferring real data, we follow recent studies [49, 30] and leverage latent generative replay. Specifically, at each communication round, we alleviate both biases – previously enforced to the last layer by the adopted prompt-based fine-tuning – by rebalancing the global classifier on a dataset of generated representations. In contrast to other approaches relying on prototypes (*i.e.*, the average feature vectors) to regularize clients’ training procedures [41, 12], we propose to compute their covariance matrix and parameterize a Multivariate Gaussian distribution for each class-client combination. This forms a grid of $\text{num_classes} \times \text{num_clients}$ generative prototypes, that are sampled hierarchically (first by class, then by client) to generate new data points.

Summarizing, this work *i*) sheds light on the relation between prompting techniques and bias, appointing the latter as the main responsible for performance degradation in Federated Class-Incremental Learning; *ii*) proposes a novel methodology that surpasses the current state-of-the-art FCIL methods on standard benchmarks while maintaining low communication costs.

2 On Federated Bias

This section investigates how Federated Bias in clients’ responses is associated with performance degradation in Federated Learning. All experiments are conducted on the CIFAR-100 [21] dataset,

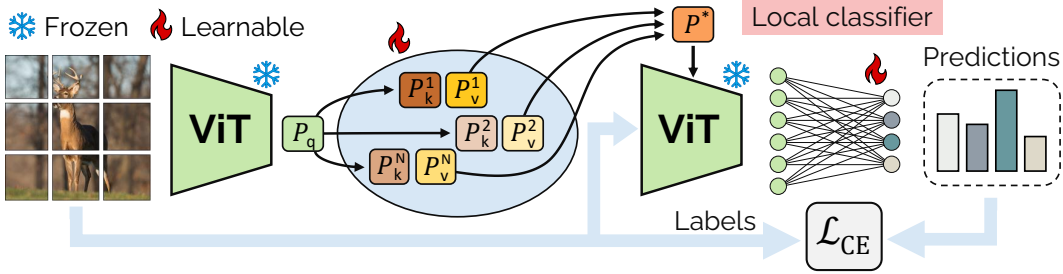


Figure 2: Client local training. P_q , P_k , and P_v stand for query, key, and value, respectively.

where the data is heterogeneously distributed across 10 clients under the commonly adopted distribution-based label imbalance [23, 47] setting.

To effectively show the existence of FB in the local models, we evaluate them at their most biased state: specifically, at the end of the local training, prior to any synchronization with the centralized server. In Figure 1 (left), we show the histogram of the responses given by two randomly selected clients, trained with $\beta = 0.05$, on the global test set. Additionally, we compare them against a model trained conventionally on the global data distribution (referred to as Joint). It can be observed that clients' predictions are significantly skewed, mirroring their local label distribution.

To define a quantitative measure for FB, we consider the responses from all clients and compute the average entropy of the histograms of their predictions. Here, low entropy indicates a highly biased model presenting a peaked response distribution, whereas high entropy implies uniformity in the model's responses and is linked to lower bias. The experiment is repeated for three increasingly challenging label-imbalance settings ($\beta \in \{0.5, 0.1, 0.05\}$). Figure 1 (right) shows the average entropy at the end of the local training compared to the final performance. The two curves are notably similar, suggesting a correlation between Federated Bias and performance deterioration.

3 Method

3.1 Problem definition

Federated Class-Incremental Learning [50, 12] tackles a classification problem across C classes, which are introduced sequentially over T incremental tasks. For each task, the data is distributed heterogeneously (*i.e.*, non-IID) among M clients. Let D^t be the global partition for task t , which is split among the M clients, with D_m^t being the local partition of client m at task t . The training procedure of each task is divided into communication rounds, each consisting of a certain number of epochs. At the end of the local optimization, the clients synchronize with the server by exchanging their learnable parameters. The server aggregates these parameters into a global model and redistributes it to all clients, thus concluding the communication round. Since data from previous tasks is unavailable, client m can only train on its dataset D_m^t during task t . Let f_{θ_m} be the local model of client m , parameterized by θ_m . The local objective is to minimize the loss function \mathcal{L} with respect to the local dataset D_m^t , namely:

$$\underset{\theta_m}{\text{minimize}} \quad \mathbb{E}_{(x,y) \sim D_m^t} \mathcal{L}(f_{\theta_m}(x), y). \quad (1)$$

The goal of the centralized server is to find the optimal set of parameters θ that minimizes the loss function on the entire dataset, without having access to any data point:

$$\underset{\theta}{\text{minimize}} \quad \frac{1}{TM} \sum_{t=1}^T \sum_{m=1}^M \mathbb{E}_{(x,y) \sim D_m^t} \mathcal{L}(f_{\theta}(x), y). \quad (2)$$

3.2 Hierarchical Generative Prototypes

In this section, we introduce our proposal, Hierarchical Generative Prototypes (HGP), which comprises two key components: i) *prompting*, reducing communication costs and constraining bias within the classifier; ii) *classifier rebalancing*, directly addressing bias on the server side. We report the pseudo-code algorithm in Appendix E.

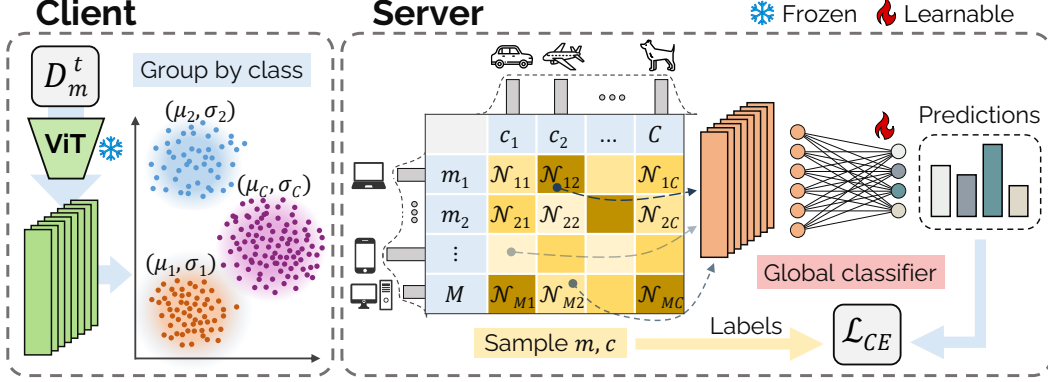


Figure 3: Classifier Rebasing procedure through hierarchical sampling.

3.2.1 Prompting

In distributed scenarios, prompting allows the use of an arbitrarily sized backbone while keeping communication costs restrained. Indeed, as most of the parameters are kept frozen, we only need to communicate the classification head and the learnable prompts. Additionally, as discussed in Section 4.3, prompting helps reducing the model’s inherent bias by confining it to the final classification layer. Let \mathcal{P} be the collection of N learnable prompts, each of which consists of a key P_k and a value P_v . For each input image, we use the pre-trained frozen backbone to extract its features h , which serve as the query P_q . Then, we compute the cosine similarity w.r.t. each prompt key, obtaining a vector of scores. These scores are then normalized, resulting in a vector $\lambda \in \mathbb{R}^N$ that is used to compute the actual prompt as $P^* = \sum_{n=1}^N \lambda^n P_v^n$ (see Figure 2). Following prefix-tuning [25, 43, 40], we prepend P^* to the keys and values of the target Multi-head Self Attention layer. After local training, each client sends its prompts and classification head of the current task t to the server. Given $|D^t| = \sum_{m=1}^M |D_m^t|$, where $|\cdot|$ represents the cardinality of a set, the server aggregates the parameters as:

$$\theta^t = \frac{1}{|D^t|} \sum_{m=1}^M |D_m^t| \theta_m^t. \quad (3)$$

Here, $\theta_m^t = \{\mathcal{P}_m^t, W_m^t\}$ indicate the learnable parameters of client m during task t (comprising of prompts \mathcal{P}_m^t and classification head W_m^t).

3.2.2 Classifier Rebasing

To generate data points for the rebasing procedure, each client m approximates the distribution of the features h related to class c with a multivariate Gaussian $\mathcal{N}_{m,c}(\mu_{m,c}, \Sigma_{m,c})$. Specifically, we compute $\mu_{m,c}$ as the mean and $\Sigma_{m,c}$ as the covariance matrix of the feature vectors produced by the local examples belonging to class c (see Figure 3, Client). Since other studies denote $\mu_{m,c}$ as the prototype for client m and class c , we refer to $\mathcal{N}_{m,c}$ as a generative prototype, given its capability to generate new samples. Thus, we obtain $M \times C$ generative prototypes, which must be combined into a single model that best approximates the global data distribution.

Tier 1 aggregation. For a given class c , the server receives M generative prototypes – one from each client – and aims to find a single distribution that best aligns with all of them. To this aim, we take the one that minimizes the Jensen-Shannon Divergence (JSD) [27]. Considering multiple distributions $\{Q_1, \dots, Q_M\}$, their JSD is defined as:

$$\text{JSD}_{\pi_1, \dots, \pi_M}(Q_1, \dots, Q_M) = \sum_{m=1}^M \pi_m D_{\text{KL}}(Q_m \parallel G), \quad G = \sum_{m=1}^M \pi_m Q_m, \quad (4)$$

where D_{KL} is the Kullback-Liebler divergence.

Therefore, our objective is to find a global distribution \tilde{Q}_c for the class c that optimizes:

$$\underset{\tilde{Q}_c}{\text{minimize}} \quad \sum_{m=1}^M \pi_{m,c} D_{\text{KL}} \left(\tilde{Q}_c \parallel G \right). \quad (5)$$

Notably, the optimal solution to this problem is to set \tilde{Q}_c equal to the distribution G . Since, in our case, all distributions $\{Q_1, \dots, Q_M\}$ are Gaussians, the closest distribution G is precisely defined as a Gaussian Mixture Model (GMM). Following a common practice in Federated Learning [41, 34], we assign the importance weights $\{\pi_{1,c}, \dots, \pi_{M,c}\}$ to each prototype based on the number of samples from each client for the class c .

Tier 2 aggregation. From the Tier 1 aggregation we obtain C GMMs $\{\tilde{Q}_1, \dots, \tilde{Q}_C\}$, one for each class. To combine them into a single model, we follow a similar reasoning to Equation 5, replacing the Gaussian distributions in Equation 4 with the resulting GMMs. Therefore, the global generative model \tilde{Q} can be defined as:

$$\tilde{Q} = \sum_{c=1}^C \omega_c \tilde{Q}_c, \quad \text{where } \tilde{Q}_c \triangleq \sum_{m=1}^M \pi_{m,c} \mathcal{N}_{m,c}(\mu_{m,c}, \Sigma_{m,c}). \quad (6)$$

To align with the label distribution of the dataset at hand, we define $\{\omega_1, \dots, \omega_C\}$ as the normalized number of samples for each class. According to Equation 5, \tilde{Q} is the distribution closest to all GMMs. Consequently, it also provides the closest match to all Gaussians across each class-client combination.

Hierarchical sampling. The standard GMM sampling process consists of two steps: selecting a Gaussian and sampling from it. Expanding on this framework, we introduce an additional step, that is used to select the class-related GMM \tilde{Q}_c from the global distribution \tilde{Q} . Specifically, as illustrated in Figure 3 (Server), our hierarchical sampling strategy draws: *i*) the GMM index c from a Multinomial on the class weights $\{\omega_1, \dots, \omega_C\}$; *ii*) the Gaussian index m from a Multinomial on the class-client weights $\{\pi_{1,c}, \dots, \pi_{M,c}\}$; *iii*) the synthetic feature \hat{h} from the multivariate Gaussian $\mathcal{N}_{m,c}$.

Rebalancing. At the conclusion of each communication round, the server blends all local generative prototypes into a hierarchical model \tilde{Q} that resembles the global distribution. Subsequently, it generates a synthetic dataset \hat{D} from \tilde{Q} . Following the aggregation of clients' learnable parameters θ_m^t according to Equation 3, the server rebalances the global classifier G parameterized by W . This is achieved by minimizing the Cross-Entropy (CE) loss w.r.t. \hat{D} :

$$\min_W \mathbb{E}_{(\hat{h}, c) \sim \hat{D}} \mathcal{L}_{\text{CE}} \left(G_W(\hat{h}), c \right). \quad (7)$$

The server redistributes the updated classifier, alongside the aggregated prompts, back to the clients, enabling them to start the subsequent communication round.

4 Experiments

In this section, we present the experimental studies utilized to assess the effectiveness of the proposed method, comparing it with the current state of the art in Federated Class-Incremental Learning.

4.1 Settings

Datasets. Following [12], we evaluated the proposed method on the CIFAR-100 [21] and Tiny-ImageNet [22] datasets. Each one is partitioned into 10 incremental tasks, resulting in 10 and 20 classes per task respectively. We distribute the data across 10 clients, employing the widely adopted *distribution-based* [23, 47] and *quantity-based* [23, 34] label imbalance settings. The former partitions the data based on a Dirichlet distribution governed by a β parameter, while the latter ensures that each client encounters exactly α classes within each task. We assess all methods across 6 scenarios for each dataset. For quantity-based label imbalance settings, we set $\alpha \in \{2, 4, 6\}$ for CIFAR-100, and $\alpha \in \{4, 8, 12\}$ for Tiny-ImageNet. On both datasets, we conduct experiments with $\beta \in \{0.05, 0.1, 0.5\}$. For all experiments, we evaluate the centralized model using the global test set.

Implementation Details. We utilize a pre-trained ViT-B/16 as the backbone for HGP and all the compared methods. Specifically, we initialize the models with supervised pre-trained weights

Table 1: **CIFAR-100 results**. Results in terms of FAA [\uparrow] and AIA [\uparrow]. AIA is reported between parenthesis. The best results are highlighted in bold. The gain refers to the previous SOTA approach.

Partition	$\beta = 0.5$	$\beta = 0.1$	$\beta = 0.05$	$\alpha = 6$	$\alpha = 4$	$\alpha = 2$
Joint	92.3					
EWC _{FL}	8.7 (24.5)	4.9 (13.1)	4.0 (11.3)	5.4 (17.8)	4.7 (14.4)	1.2 (6.8)
LwF _{FL}	16.3 (35.8)	7.7 (17.8)	7.7 (14.9)	11.4 (24.6)	10.3 (19.4)	3.0 (9.3)
iCaRL _{FL}	54.8 (63.7)	48.2 (53.5)	42.9 (43.8)	42.2 (48.6)	38.5 (42.3)	26.8 (28.3)
L2P _{FL}	77.4 (83.3)	71.3 (79.4)	69.4 (77.0)	72.8 (80.3)	70.4 (79.2)	63.4 (72.0)
CODA-P _{FL}	61.3 (71.8)	18.1 (35.4)	15.9 (34.3)	35.2 (50.0)	15.1 (34.6)	27.7 (9.5)
TARGET	13.3 (33.8)	1.2 (13.6)	4.0 (12.7)	6.4 (23.9)	5.7 (18.7)	1.6 (8.2)
GLFC	– (–)	– (–)	– (–)	50.0 (66.9)	50.5 (61.0)	4.4 (12.5)
LGA	– (–)	– (–)	– (–)	62.9 (73.5)	61.4 (67.5)	9.8 (15.1)
PLoRA	79.3 (85.9)	78.2 (84.6)	77.8 (84.5)	79.2 (85.3)	77.4 (83.7)	73.2 (81.1)
HGP (ours)	89.3 (92.9)	88.7 (92.4)	88.9 (92.5)	89.4 (92.8)	88.5 (91.9)	88.1 (91.6)
Gain	10.0 (7.0)	10.5 (7.8)	11.1 (8.0)	10.2 (7.5)	11.1 (8.2)	14.9 (10.5)

on ImageNet-21K [38] for CIFAR-100 and self-supervised pre-trained weights of DINO [3] for Tiny-ImageNet. This choice is grounded on mitigating potential data leakage when adapting the model to the latter dataset, which is a subset of ImageNet [6]. For a complete overview of all the hyperparameters, refer to Appendix B.1. Results are averaged across 3 runs.

4.2 Results

Metrics. We assess the performance of all methods using two widely adopted metrics in FCIL literature: Final Average Accuracy (FAA) and Average Incremental Accuracy (AIA). For the mathematical definitions of these measures, we refer the reader to Appendix B.2. **Evaluated approaches.** Our proposal is evaluated alongside nine competitors, following the methodology outlined in [12]. Among these competitors, five were originally designed for Class-Incremental Learning and adapted to the federated setting by aggregating decentralized models using the FedAvg algorithm [34]. Specifically, we include two regularization-based techniques (EWC [20], LwF [26]), one leveraging a rehearsal buffer (iCaRL [37]), and two prompting-based approaches (L2P [44], CODA-Prompt [40]). Conversely, the remaining four algorithms are specifically tailored for Federated Class-Incremental Learning. These include a Parameter-Efficient Fine-Tuning technique (PLoRA [12]), two rehearsal-based methods (GLFC [9] and LGA [8]), and one utilizing generative replay (TARGET [50]). Results for all methods, except HGP and CODA-Prompt, are sourced from previous research [12]. Additionally, we include the upper bound, established by training the same backbone jointly on the global data distribution (*i.e.*, without applying any kind of federated or incremental splitting), referred to as Joint.

Comparison. In Tables 1 and 2, we present the results of HGP and the other approaches in terms of FAA [\uparrow] and AIA [\uparrow] on the CIFAR-100 and Tiny-ImageNet datasets, respectively. Generally, all methods tested on Tiny-ImageNet (including Joint) exhibit lower performance compared to CIFAR-100, indicating the greater challenge posed by the former dataset. Consistent with previous findings [42, 2], regularization techniques for CIL (EWC, LwF) perform poorly across all imbalance levels, indicating severe forgetting issues during incremental learning. iCaRL is less effective compared to prompting techniques like L2P and CODA-Prompt on more balanced datasets. However, thanks to the presence of a memory buffer of old samples, it maintains relatively consistent results as label imbalance increases. While L2P generally outperforms CODA-Prompt, its performance remains lower than PEFT-based methods designed specifically for FCIL. For further insights on L2P results, we refer the reader to the Appendix C.

Among FCIL methods, TARGET exhibits the lowest performance. Notably, it exhibits significantly higher AIA compared to FAA, suggesting ineffective mitigation of forgetting through its generative replay. GLFC and LGA perform better than iCaRL but worse than prompting techniques, indicating the improved effectiveness of their class-aware gradient compensation compared to relying solely on

Table 2: **Tiny-ImageNet results.** Results in terms of FAA [\uparrow] and AIA [\uparrow]. AIA is reported between parenthesis. The best results are highlighted in bold. The gain refers to the previous SOTA approach.

Partition	$\beta = 0.5$	$\beta = 0.1$	$\beta = 0.05$	$\alpha = 12$	$\alpha = 8$	$\alpha = 4$
Joint				83.2		
L2P _{FL}	64.2 (66.9)	56.3 (52.5)	51.9 (43.2)	61.6 (58.0)	49.4 (39.3)	8.2 (10.2)
CODA-P _{FL}	72.2 (81.1)	54.4 (64.2)	45.6 (57.9)	64.3 (75.1)	49.9 (62.2)	27.1 (42.8)
TARGET	7.7 (20.5)	0.5 (8.7)	0.9 (5.3)	3.5 (17.6)	4.1 (16.4)	0.5 (4.8)
GLFC	– (–)	– (–)	– (–)	35.0 (47.9)	20.2 (37.5)	5.1 (8.7)
LGA	– (–)	– (–)	– (–)	37.3 (53.2)	61.4 (67.5)	6.5 (9.8)
PLoRA	75.5 (81.8)	74.3 (81.0)	74.1 (80.7)	75.3 (81.7)	75.2 (81.6)	73.6 (80.1)
HGP (ours)	79.3 (85.0)	79.3 (85.0)	78.7 (84.6)	79.6 (85.1)	79.3 (84.9)	79.2 (84.8)
Gain	3.8 (3.2)	5.0 (4.0)	4.6 (3.9)	4.3 (3.4)	3.9 (3.3)	5.6 (4.7)

a memory buffer. However, both methods struggle with highly imbalanced label distributions. Due to computing constraints, we omit to report the performance of GLFC and LGA on distribution-based label imbalance settings.

PEFT-based methods (PLoRA, HGP) outperform other methodologies across all settings. The use of prototypes enables them to handle increasing label imbalance more effectively, resulting in the most stable performance among variations in α and β in both datasets. HGP significantly outperforms PLoRA in all scenarios by leveraging generative prototypes on the centralized server, demonstrating superior robustness to both incremental and federated biases. Notably, HGP approaches the Joint upper bound (*i.e.*, $\Delta = 2.9\%$ for $\alpha = 6$ on CIFAR-100, and $\Delta = 3.6\%$ for $\alpha = 12$ on Tiny-ImageNet), demonstrating a remarkable resilience to any form of imbalance or forgetting.

4.3 Ablation study

Prompting vs. Fine-Tuning. In this section, we explore the impact of prompting on Federated Bias, emphasizing the contrast with the traditional approach of fine-tuning the whole network. All experiments are performed on the CIFAR-100 dataset, distributed across 10 clients under different distribution-based label imbalance settings.

We argue that prompting is a more advantageous approach for adapting pre-trained models in Federated Learning, as it constrains the bias to the last layer instead of distributing it across the whole network. To experimentally prove this claim, we position ourselves at the end of the local training prior to the first synchronization with the server: namely, when each client is trained exclusively on its local distribution. In this scenario, we compute the local prototypes for each client and measure their pairwise Euclidean distance, averaged on the 10 clients. Figure 4 (left) shows that prompting results in smaller feature bias compared to traditional Fine-Tuning (FT), suggesting that the obtained features are, on average, less biased towards the local distributions. To validate this assertion, we also compute the same metric on the pre-trained model (ViT-B-16 on ImageNet-21k), which yields the smallest bias by design. This further supports our reasoning, as this last network experiences no fine-tuning whatsoever.

On the right-hand side of Figure 4, we show the performance of prompting *vs.* traditional fine-tuning. In line with recent works [49, 36, 33], prompting (Prompt) shows inferior performance compared to Fine-Tuning (FT), due to its limited plasticity. However, when leveraging Classifier Rebalancing (CR) on both approaches, we observe a reversal in this trend. Notably, simply addressing Federated Bias in the last layer is sufficient for prompting to outperform classical fine-tuning: this suggests that prompting techniques train more biased classifiers while producing less biased features, effectively restricting FB to the final layer.

Impact of Different Components. We assess the specific contributions of various components of HGP in terms of FAA for both benchmarks under one distribution-based label imbalance setting with $\beta = 0.05$. Results of these ablative experiments are summarized in Table 3.

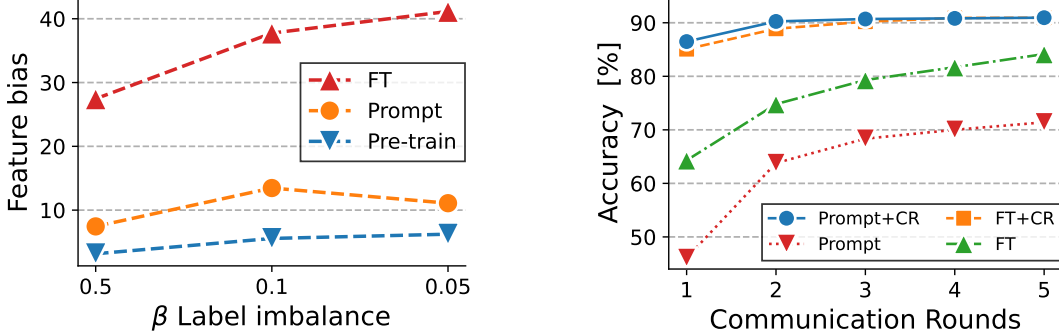


Figure 4: **Prompting vs. Fine-tuning.** Average pairwise distance of the local prototypes on all clients (left). FL performance before and after Classifier Rebalancing (CR), for $\beta = 0.05$ (right).

Table 3: **HGP components.** Evaluation of the singular components of HGP in terms of FAA [↑].

Prompting	CR _{old}	CR _{cur}	CIFAR-100	Tiny-ImageNet
✗	✗	✗	44.8	38.7
✓	✗	✗	51.8	43.5
✓	✓	✗	81.7	70.7
✓	✗	✓	77.8	69.8
✓	✓	✓	88.9	78.7

Starting with the full Fine-Tuning of ViT-B/16 serves as a lower bound. Incorporating our prompting technique yields a notable improvement. It is worth noting that the primary advantage of prompting lies not only in enhancing accuracy but also in confining bias to the final classification layer, thereby facilitating Classifier Rebalancing.

We denote CR_{cur} and CR_{old} as the classifier rebalancing procedure applied to the current task classes and the old tasks classes, respectively. Specifically, CR_{cur} rebalances the classifier with features generated from prototypes belonging to the set of classes of the current task, while CR_{old} employs sampling on the set of classes of the old tasks. The latter exhibits a greater improvement compared to the former, indicating the greater importance of addressing Incremental Bias.

By integrating all these components, HGP achieves state-of-the-art performance as reported in Tables 1 and 2.

5 Relation with prior works

Federated Learning. In its most naive form, Federated Learning suggests combining local models at the conclusion of each round through parameters averaging [34]. Other approaches introduce regularization techniques during local models training to prevent them from drifting too far from the server’s parameter space. For instance, FedProx [24] and SCAFFOLD [16] enforce such regularization. FedDC [11] estimates the local parameter shift and employs it as a correction term before aggregating parameters. GradMA [29] addresses optimization challenges (*i.e.*, quadratic programming) by rerouting each client update towards optimizing the local problem while maintaining proximity to the server. On a different trajectory, FedProto [41] computes prototypes for each class observed by each client, which are then aggregated by the server into global prototypes, serving as target representations for subsequent rounds. Similarly, in [30], the authors fit Gaussian distributions for each class and use them to generate an IID dataset of features, subsequently calibrating the server’s classification head with these features. In our work, we leverage hierarchical Gaussian Mixture Models (GMMs) of prototypes and sample from them to rebalance the global classifier.

Class-Incremental Learning. Class-Incremental Learning (CIL) stands out as one of the most challenging settings within the Continual Learning domain [42]. In this scenario, the training process

is divided into distinct tasks, each introducing new classes as the training progresses. To address this setting, early methods rely on regularization techniques, establishing checkpoints for previous tasks and aiming to maintain proximity to w.r.t. their parameters [48, 20] or predictions [26]. Alternatively, rehearsal-based approaches involve storing samples in a limited memory buffer and subsequently replaying them to optimize either the original objective [39, 4] or a different one based on knowledge distillation [37, 2]. The emergence of pre-trained self-attentive architectures [10] in the Computer Vision domain has paved the way for significant advancements, particularly with the advent of Parameter-Efficient Fine-Tuning (PEFT) techniques. Notably, recent approaches [44, 43, 40] have harnessed prompting to achieve state-of-the-art performance in CIL, eliminating the need for a buffer to replay old samples. Instead, they employ a prompt pool comprising incrementally learned prompts, utilized to condition the network during the forward pass. In our method, we embrace the prompting paradigm, which not only delivers robust performance but also facilitates efficient communication rounds in terms of exchanged parameters.

Federated Class-Incremental Learning. The concept of Federated Class-Incremental Learning (FCIL) was initially introduced in [46]. In their work, the authors propose FedWeIT, which partitions client-side parameters into task-generic and task-specific components. To mitigate interference between clients, they implement sparse learnable masks to selectively extract relevant knowledge for each client. GLFC [9] takes a different approach by combining local buffers with class-aware gradient compensation loss. This strategy helps counteract catastrophic forgetting through rehearsal, while also adjusting the magnitude of gradient updates based on whether input samples belong to new or old classes. Building upon this framework, an enhanced version is introduced by the same authors in the LGA paper [8]. TARGET [50] tackles forgetting by training a centralized generator network to produce synthetic data, maintaining a similar behavior to the generator used in previous tasks. The generative network populates a buffer after each task, allowing clients to utilize it for rehearsal. Recent advancements in FCIL involve fine-tuning pre-trained models using PEFT techniques. Fed-CPrompt [1] introduces a regularization term that encourages local prompts to diverge from global ones, enabling them to learn task-specific features. Meanwhile, PLORA [12] integrates LoRA [13] with prototypes, which are aggregated via a re-weighting mechanism on the server side during each communication round. As a result, clients leverage these aggregated prototypes as target representations to govern local training.

6 Conclusions

In this work, we propose Hierarchical Generative Prototypes (HGP), an approach aimed at mitigating Incremental and Federated Biases within Federated Class-Incremental Learning. HGP utilizes pre-trained architectures conditioned by prompting to achieve communication efficiency. We examine the bias implications of fine-tuning the entire model compared to using prompting techniques, demonstrating that prompting confines the bias primarily to the classification layer. Building on these insights, we propose Classifier Rebalancing as a solution. This method involves sampling features from a hierarchical Gaussian Mixture Model to train the classifier across all observed classes, effectively reducing bias in the classification layer. Through the integration of prompt learning and classifier rebalancing, we achieve superior performance compared to the state-of-the-art while transmitting only a minimal number of parameters.

Limitations and broader impact

This work effectively tackles typical FCIL challenges such as communication costs and privacy concerns. However, a potential limitation could arise from the reliance on pre-trained models, although this practice is widely accepted in federated literature [12, 28, 1]. Another limitation could stem from the use of datasets that are in distribution with the pretraining data.

We believe that Federated Class-Incremental Learning plays a crucial role in a world where edge devices are increasingly pervasive. The ability to learn online while leveraging distributed knowledge is of significant importance for advancing the field of Machine Learning. With our work, which achieves state-of-the-art performance in this domain, we aim to stimulate further research and advancements in federated and continual learning.

References

- [1] Gaurav Bagwe, Xiaoyong Yuan, Miao Pan, and Lan Zhang. Fed-cprompt: Contrastive prompt for rehearsal-free federated continual learning. In *Federated Learning and Analytics in Practice: Algorithms, Systems, Applications, and Opportunities*, 2023.
- [2] Pietro Buzzega, Matteo Boschini, Angelo Porrello, Davide Abati, and Simone Calderara. Dark experience for general continual learning: a strong, simple baseline. *Advances in Neural Information Processing Systems*, 2020.
- [3] Mathilde Caron, Hugo Touvron, Ishan Misra, Hervé Jégou, Julien Mairal, Piotr Bojanowski, and Armand Joulin. Emerging properties in self-supervised vision transformers. In *IEEE International Conference on Computer Vision*, 2021.
- [4] Arslan Chaudhry, Marcus Rohrbach, Mohamed Elhoseiny, Thalaiyasingam Ajanthan, P Dokania, P Torr, and M Ranzato. Continual learning with tiny episodic memories. In *Workshop on Multi-Task and Lifelong Reinforcement Learning*, 2019.
- [5] Liam Collins, Hamed Hassani, Aryan Mokhtari, and Sanjay Shakkottai. Exploiting shared representations for personalized federated learning. In *International Conference on Machine Learning*, 2021.
- [6] Jia Deng, Wei Dong, Richard Socher, Li-Jia Li, Kai Li, and Li Fei-Fei. Imagenet: A large-scale hierarchical image database. In *Proceedings of the IEEE Conference on Computer Vision and Pattern Recognition*, 2009.
- [7] Enmao Diao, Jie Ding, and Vahid Tarokh. Heterofl: Computation and communication efficient federated learning for heterogeneous clients. In *International Conference on Learning Representations*, 2021.
- [8] Jiahua Dong, Hongliu Li, Yang Cong, Gan Sun, Yulun Zhang, and Luc Van Gool. No one left behind: Real-world federated class-incremental learning. *IEEE Transactions on Pattern Analysis and Machine Intelligence*, 2023.
- [9] Jiahua Dong, Lixu Wang, Zhen Fang, Gan Sun, Shichao Xu, Xiao Wang, and Qi Zhu. Federated class-incremental learning. In *Proceedings of the IEEE Conference on Computer Vision and Pattern Recognition*, 2022.
- [10] Alexey Dosovitskiy, Lucas Beyer, Alexander Kolesnikov, Dirk Weissenborn, Xiaohua Zhai, Thomas Unterthiner, Mostafa Dehghani, Matthias Minderer, Georg Heigold, Sylvain Gelly, et al. An image is worth 16x16 words: Transformers for image recognition at scale. In *International Conference on Learning Representations*, 2020.
- [11] Liang Gao, Huazhu Fu, Li Li, Yingwen Chen, Ming Xu, and Cheng-Zhong Xu. Feddc: Federated learning with non-iid data via local drift decoupling and correction. In *Proceedings of the IEEE Conference on Computer Vision and Pattern Recognition*, 2022.
- [12] Haiyang Guo, Fei Zhu, Wenzhuo Liu, Xu-Yao Zhang, and Cheng-Lin Liu. Federated class-incremental learning with prototype guided transformer. *arXiv preprint arXiv:2401.02094*, 2024.
- [13] Edward J Hu, Phillip Wallis, Zeyuan Allen-Zhu, Yuanzhi Li, Shean Wang, Lu Wang, Weizhu Chen, et al. Lora: Low-rank adaptation of large language models. In *International Conference on Learning Representations*, 2021.
- [14] Fatih Ilhan, Gong Su, and Ling Liu. Scalefl: Resource-adaptive federated learning with heterogeneous clients. In *Proceedings of the IEEE Conference on Computer Vision and Pattern Recognition*, 2023.
- [15] Dahuin Jung, Dongyoon Han, Jihwan Bang, and Hwanjun Song. Generating instance-level prompts for rehearsal-free continual learning. In *IEEE International Conference on Computer Vision*, 2023.
- [16] Sai Praneeth Karimireddy, Satyen Kale, Mehryar Mohri, Sashank Reddi, Sebastian Stich, and Ananda Theertha Suresh. Scaffold: Stochastic controlled averaging for federated learning. In *International Conference on Machine Learning*, 2020.
- [17] Gyuhak Kim, Changnan Xiao, Tatsuya Konishi, Zixuan Ke, and Bing Liu. A theoretical study on solving continual learning. *Advances in Neural Information Processing Systems*, 2022.

- [18] Minjae Kim, Sangyoon Yu, Suhyun Kim, and Soo-Mook Moon. Depthfl: Depthwise federated learning for heterogeneous clients. In *International Conference on Learning Representations*, 2022.
- [19] Diederik Kingma and Jimmy Ba. Adam: A method for stochastic optimization. In *International Conference on Learning Representations*, 2015.
- [20] James Kirkpatrick, Razvan Pascanu, Neil Rabinowitz, Joel Veness, Guillaume Desjardins, Andrei A Rusu, Kieran Milan, John Quan, Tiago Ramalho, Agnieszka Grabska-Barwinska, et al. Overcoming catastrophic forgetting in neural networks. *Proceedings of the National Academy of Sciences*, 2017.
- [21] Alex Krizhevsky, Geoffrey Hinton, et al. Learning multiple layers of features from tiny images. *Master's thesis, Department of Computer Science, University of Toronto*, 2009.
- [22] Ya Le and Xuan Yang. Tiny imagenet visual recognition challenge. *CS 231N*, 2015.
- [23] Qinbin Li, Yiqun Diao, Quan Chen, and Bingsheng He. Federated learning on non-iid data silos: An experimental study. In *IEEE International Conference on Data Engineering*, 2022.
- [24] Tian Li, Anit Kumar Sahu, Manzil Zaheer, Maziar Sanjabi, Ameet Talwalkar, and Virginia Smith. Federated optimization in heterogeneous networks. *Proceedings of Machine Learning and Systems*, 2020.
- [25] Xiang Lisa Li and Percy Liang. Prefix-tuning: Optimizing continuous prompts for generation. In *Proceedings of the International Joint Conference on Natural Language Processing*, 2021.
- [26] Zhizhong Li and Derek Hoiem. Learning without forgetting. *IEEE Transactions on Pattern Analysis and Machine Intelligence*, 2017.
- [27] Jianhua Lin. Divergence measures based on the shannon entropy. *IEEE Transactions on information theory*, 1991.
- [28] Chenghao Liu, Xiaoyang Qu, Jianzong Wang, and Jing Xiao. Fedet: a communication-efficient federated class-incremental learning framework based on enhanced transformer. In *International Joint Conference on Artificial Intelligence*, 2023.
- [29] Kangyang Luo, Xiang Li, Yunshi Lan, and Ming Gao. Gradma: A gradient-memory-based accelerated federated learning with alleviated catastrophic forgetting. In *Proceedings of the IEEE Conference on Computer Vision and Pattern Recognition*, 2023.
- [30] Mi Luo, Fei Chen, Dapeng Hu, Yifan Zhang, Jian Liang, and Jiashi Feng. No fear of heterogeneity: Classifier calibration for federated learning with non-iid data. *Advances in Neural Information Processing Systems*, 2021.
- [31] Xiaosong Ma, Jie Zhang, Song Guo, and Wenchao Xu. Layer-wised model aggregation for personalized federated learning. In *Proceedings of the IEEE Conference on Computer Vision and Pattern Recognition*, 2022.
- [32] Michael McCloskey and Neal J Cohen. Catastrophic interference in connectionist networks: The sequential learning problem. In *Psychology of learning and motivation*, 1989.
- [33] Mark D McDonnell, Dong Gong, Amin Parvaneh, Ehsan Abbasnejad, and Anton van den Hengel. Ranpac: Random projections and pre-trained models for continual learning. *Advances in Neural Information Processing Systems*, 2024.
- [34] Brendan McMahan, Eider Moore, Daniel Ramage, Seth Hampson, and Blaise Aguera y Arcas. Communication-efficient learning of deep networks from decentralized data. In *International Conference on Artificial Intelligence and Statistics*, 2017.
- [35] JAE HOON OH, Sangmook Kim, and Seyoung Yun. Fedbabu: Toward enhanced representation for federated image classification. In *International Conference on Learning Representations*, 2022.
- [36] Aristeidis Panos, Yuriko Kobe, Daniel Olmeda Reino, Rahaf Aljundi, and Richard E Turner. First session adaptation: A strong replay-free baseline for class-incremental learning. In *IEEE International Conference on Computer Vision*, 2023.
- [37] Sylvestre-Alvise Rebuffi, Alexander Kolesnikov, Georg Sperl, and Christoph H Lampert. icarl: Incremental classifier and representation learning. In *Proceedings of the IEEE Conference on Computer Vision and Pattern Recognition*, 2017.

[38] Tal Ridnik, Emanuel Ben-Baruch, Asaf Noy, and Lihi Zelnik-Manor. Imagenet-21k pretraining for the masses. In *Conference on Neural Information Processing Systems Datasets and Benchmarks Track (Round 1)*, 2021.

[39] Anthony Robins. Catastrophic forgetting, rehearsal and pseudorehearsal. *Connection Science*, 1995.

[40] James Seale Smith, Leonid Karlinsky, Vyshnavi Gutta, Paola Cascante-Bonilla, Donghyun Kim, Assaf Arbelle, Rameswar Panda, Rogerio Feris, and Zsolt Kira. Coda-prompt: Continual decomposed attention-based prompting for rehearsal-free continual learning. In *Proceedings of the IEEE Conference on Computer Vision and Pattern Recognition*, 2023.

[41] Yue Tan, Guodong Long, Lu Liu, Tianyi Zhou, Qinghua Lu, Jing Jiang, and Chengqi Zhang. Fedproto: Federated prototype learning across heterogeneous clients. In *Proceedings of the AAAI Conference on Artificial Intelligence*, 2022.

[42] Gido M. van de Ven, Tinne Tuytelaars, and Andreas Savas Tolias. Three types of incremental learning. *Nature Machine Intelligence*, 2022.

[43] Zifeng Wang, Zizhao Zhang, Sayna Ebrahimi, Ruoxi Sun, Han Zhang, Chen-Yu Lee, Xiaoqi Ren, Guolong Su, Vincent Perot, Jennifer Dy, et al. Dualprompt: Complementary prompting for rehearsal-free continual learning. In *Proceedings of the European Conference on Computer Vision*, 2022.

[44] Zifeng Wang, Zizhao Zhang, Chen-Yu Lee, Han Zhang, Ruoxi Sun, Xiaoqi Ren, Guolong Su, Vincent Perot, Jennifer Dy, and Tomas Pfister. Learning to prompt for continual learning. In *Proceedings of the IEEE Conference on Computer Vision and Pattern Recognition*, 2022.

[45] Yue Wu, Yinpeng Chen, Lijuan Wang, Yuancheng Ye, Zicheng Liu, Yandong Guo, and Yun Fu. Large scale incremental learning. In *Proceedings of the IEEE Conference on Computer Vision and Pattern Recognition*, 2019.

[46] Jaehong Yoon, Wonyong Jeong, Giwoong Lee, Eunho Yang, and Sung Ju Hwang. Federated continual learning with weighted inter-client transfer. In *International Conference on Machine Learning*, 2021.

[47] Mikhail Yurochkin, Mayank Agarwal, Soumya Ghosh, Kristjan Greenewald, Nghia Hoang, and Yasaman Khazaeni. Bayesian nonparametric federated learning of neural networks. In *International Conference on Machine Learning*, 2019.

[48] Friedemann Zenke, Ben Poole, and Surya Ganguli. Continual learning through synaptic intelligence. In *International Conference on Machine Learning*, 2017.

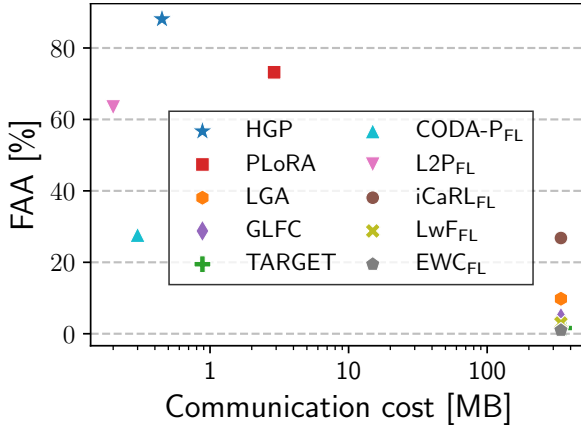
[49] Gengwei Zhang, Liyuan Wang, Guoliang Kang, Ling Chen, and Yunchao Wei. Slca: Slow learner with classifier alignment for continual learning on a pre-trained model. In *IEEE International Conference on Computer Vision*, 2023.

[50] Jie Zhang, Chen Chen, Weiming Zhuang, and Lingjuan Lyu. Target: Federated class-continual learning via exemplar-free distillation. In *IEEE International Conference on Computer Vision*, 2023.

[51] Haodong Zhao, Wei Du, Fangqi Li, Peixuan Li, and Gongshen Liu. Fedprompt: Communication-efficient and privacy-preserving prompt tuning in federated learning. In *IEEE International Conference on Acoustics, Speech and Signal Processing*, 2023.

[52] Nanxuan Zhao, Zhirong Wu, Rynson WH Lau, and Stephen Lin. What makes instance discrimination good for transfer learning? In *International Conference on Learning Representations*, 2020.

A Communication cost



Methods	$C \rightarrow S$	$S \rightarrow C$
EWC _{FL}	340.7	340.7
LwF _{FL}	340.7	340.7
iCaRL _{FL}	340.7	340.7
L2P _{FL}	0.2	0.2
CODA-P _{FL}	0.3	0.3
TARGET	340.7	377.5
GLFC	340.7	340.7
LGA	340.7	340.7
PLoRA	2.9	2.9
HGP (ours)	0.3	0.6

Figure 5: FAA [%] in relation with the communication cost [MB] for all the tested approaches (left). Communication costs for client-server ($C \rightarrow S$) and server-client communications ($S \rightarrow C$), for each communication round (right).

Efficient communication is essential in Federated Learning because of the extensive coordination required between server and clients. In this section, we analyze the communication cost for each tested method. Figure 5 (left) illustrates the relationship between Final Average Accuracy (FAA) and communication cost for each method. The FAA results are derived from a quantity-based scenario with $\alpha = 2$ on CIFAR-100. The communication cost – reported in Megabytes (MB) for each communication round – is calculated as the average amount of data exchanged from a single client to the server ($C \rightarrow S$) and from the server to a single client ($S \rightarrow C$). The specific values are reported in Figure 5 (right).

Notably, methods that do not utilize PEFT techniques incur significantly higher communication costs, as they optimize all parameters. Consequently, with larger models, communication costs escalate proportionally without corresponding performance gains. TARGET is the most expensive method overall because the server sends the entire model and the generated dataset to clients once per task. In contrast, the adoption of PEFT techniques enhances both efficiency and performance. L2P emerges as the most efficient method, using fewer prompts than its competitors. CODA-P transmits slightly more parameters than L2P. However, by only sending prompts for the current task and keeping the others frozen, it maintains comparable communication costs.

Although PLoRA is less efficient than prompt-based methods due to the larger size of LoRA modules, it still achieves costs that are two orders of magnitude lower than fine-tuning approaches while delivering superior performance. HGP demonstrates efficiency on par with the other prompt-based techniques, with slightly higher server-client communication cost. This is attributed to the Classifier Rebalancing process, which also changes the classification heads related to the previous tasks, thus necessitating to communicate the whole updated classifier back to the clients.

Overall, the efficiency gains and substantial performance improvements offered by PEFT techniques highlight their advantage in Federated Learning scenarios.

B Implementation details

B.1 Hyperparameters

We utilize a pre-trained ViT-B/16 as the backbone for HGP and all the compared methods. Specifically, we initialize the models with supervised pre-trained weights on ImageNet-21K [38] for CIFAR-100 and self-supervised pre-trained weights from DINO [3] for Tiny-ImageNet. This selection is made to mitigate potential data leakage when adapting the model to the latter dataset, which is a subset of ImageNet [6].

In our method, we adopt a prompt pool composed of 10 prompts for each task. Across all experiments, prompt components have a shape of $(8, d)$, where $d = 768$ represents the embedding dimension for the chosen architecture. We apply these prompts using prefix tuning, conditioning the first 5 layers of the backbone. For each task, we perform five communication rounds, during which clients observe their local datasets for five epochs with a batch size of 64. Training is conducted using the Adam optimizer [19] with a learning rate of 0.001; β_1 and β_2 are set to 0.9 and 0.999, respectively. A cosine annealing scheduler is employed to decay the learning rate during local training.

The centralized server rebalances the global classifier for five epochs. We use the SGD optimizer with a learning rate of 0.01 and a momentum of 0.9, with a batch size of 256, and also apply a cosine annealing learning rate scheduler. We generate an average of 256 feature vectors for each class encountered up to this point, multiplying the covariance associated with each prototype by 3 to enhance dataset diversity. All images are resized to 224×224 using bicubic interpolation and scaled to ensure their values fall within the range $[0, 1]$. Additionally, we employ random cropping and horizontal flipping as data augmentation techniques.

All experiments are conducted using 1 Nvidia RTX5000 GPU.

B.2 Metrics

We assess the performance of all methods using two widely adopted metrics in FCIL literature: Final Average Accuracy (FAA) and Average Incremental Accuracy (AIA).

FAA represents the mean accuracy on all observed tasks at the conclusion of the incremental training process. Mathematically, if A_i^j denotes the accuracy on the i^{th} task at the j^{th} incremental step, where $i \leq j$, FAA can be expressed as:

$$\text{FAA} = \frac{1}{T} \sum_{i=1}^T A_i^T. \quad (8)$$

On the other hand, AIA provides insight into the performance progression throughout the training process. It calculates the average accuracy after each task, considering all data encountered up to that point. After completion of the entire training procedure, the mean of all measurements is computed as follows:

$$\text{AIA} = \frac{1}{T} \sum_{j=1}^T \left[\frac{1}{j} \sum_{i=1}^j A_i^j \right]. \quad (9)$$

C Batch-wise prompting

Table 4: **Batch-wise prompting.** FAA \uparrow and AIA \uparrow for L2P, with and without batch-wise prompting at test time on all settings. AIA is reported between parenthesis.

Partition	$\beta = 0.5$	$\beta = 0.1$	$\beta = 0.05$	$\alpha = 6$	$\alpha = 4$	$\alpha = 2$
Dataset						
				CIFAR-100		
L2P _{FL} (BP)	77.4 (83.3)	71.3 (79.4)	69.4 (77.0)	72.8 (80.3)	70.4 (79.2)	63.4 (72.0)
L2P _{FL}	80.0 (83.7)	47.9 (57.7)	43.2 (52.1)	49.8 (60.1)	25.2 (41.9)	10.0 (24.3)
Dataset						
				Tiny-ImageNet		
L2P _{FL} (BP)	64.2 (66.9)	56.3 (52.5)	51.9 (43.2)	61.6 (58.0)	49.4 (39.3)	8.2 (10.2)
L2P _{FL}	60.3 (70.8)	42.2 (50.6)	36.5 (45.4)	51.4 (61.5)	26.8 (43.0)	7.5 (13.1)

To maintain consistency with other studies, we report L2P performance (Tables 1 and 2) using Batch-wise Prompting (BP) at test time [15, 40]. Such a procedure involves selecting the same set of prompts for all samples within a single batch during testing, thus violating the test assumption

of processing each sample independently. This gives L2P an unfair advantage compared to other methods when the test dataset is not shuffled: *i.e.*, when the ground-truth labels of the examples within a single batch are typically the same.

In this respect, Table 4 presents L2P’s performance with and without batch-wise prompting. Without BP, the set of prompts is selected individually for each sample, ensuring independent predictions. L2P achieves similar results with and without batch-wise prompting when $\beta = 0.5$. However, in all the other settings, batch-wise prompting appears to increment L2P’s performance considerably, especially on CIFAR-100.

D Prototypes of features are privacy-preserving

In Federated Learning, maintaining the privacy of local data distributions is of utmost importance. It is crucial that no private samples are directly transmitted from the client to the server. In the HGP framework, each client provide the server with a generative prototype for each observed class.

To verify the safety of generative prototypes, we firstly examine a hypothetical scenario where an attacker gains access to the trained model along with a real image utilized during training. In such a case, the attacker could potentially employ the feature inversion technique outlined in [52]. This methodology provides for training a autoencoder to precisely match the input image. Specifically, the autoencoder takes fixed noise as input and reconstructs the image. Then, both the real and reconstructed image are passed through the frozen backbone. The objective is to minimize the mean squared error (MSE) loss between their respective features. Figure 6 (left) shows the real training image from the Tiny-ImageNet dataset, while Figure 6 (center) displays the reconstruction obtained by the trained autoencoder. Through this process, no significant semantics can be recovered. At most, the class might be guessed, but the image does not provide any detail of the original sample.

In another setting, we suppose that the attacker gains access to the centralized server, which has visibility into clients’ generative prototypes. To recover an input image, initial random noise in the input space is optimized by minimizing MSE between its features and those of a fixed sample from the generative prototype. Figure 6 (right) shows that this results in a shapeless, noisy reconstruction, making it impracticable for an attacker to recreate real images from these feature distributions.



Figure 6: Real training image (left) and its reconstructions leveraging either the input image (center) or the generative prototype of the related class (right).

E Algorithm

Algorithm 1 Hierarchical Generative Prototypes **HGP**

```

1: Input: generic task  $t$ ;  $M$  clients; local model  $f_{\theta_m^t}(\cdot)$  parameterized by  $\theta_m^t = \{\mathcal{P}_m^t, W_m^t\}$ ;  

    $N$  prompts;  $C$  classes;  $E$  local epochs;  $E_r$  rebalancing epochs; local learning rate  $\eta$ ;  

   rebalancing learning rate  $\eta_r$ .  

2: for each communication round do  

3:   Server side:  

4:     Server distributes  $\theta^t$   

5:     Client side:  

6:     for each client  $m \in \{1, \dots, M\}$  in parallel do  

7:        $\theta_m^t = \theta^t$   

8:       for each local epoch  $e \in \{1, \dots, E\}$  do  

9:         for each batch  $(x, y) \sim D_m^t$  do  

10:          Compute query  $P_q$   

11:          Compute similarities  $\lambda^n = \text{cosine\_similarity}(P_q, P_k^n) \ \forall n \in \{1, \dots, N\}$   

12:          Compute prompt  $P^* = \sum_{n=1}^N \lambda^n P_v^n$   

13:           $\theta_m^t \leftarrow \theta_m^t - \eta \nabla \mathcal{L}_{\text{CE}}(f_{\theta_m^t}(x), y)$   

14:        end for  

15:      end for  

16:      Compute feature vectors  $h$  on  $D_m^t$   

17:      for each class  $c \in C^t$  do  

18:        Compute  $\mu_{m,c}$  and  $\Sigma_{m,c}$  to parameterize  $\mathcal{N}_{m,c}$   

19:      end for  

20:      Send parameters  $\theta_m^t$  and Gaussians  $\mathcal{N}_{m,c}$  to the server  

21:    end for  

22:    Server side:  

23:    Compute  $\theta^t = \frac{1}{|D^t|} \sum_{m=1}^M |D_m^t| \theta_m^t$   

24:    for each class  $c \in C^t$  do  

25:      Compute  $\tilde{Q}_c = \sum_{m=1}^M \pi_{m,c} \mathcal{N}_{m,c}(\mu_{m,c}, \Sigma_{m,c})$   

26:    end for  

27:    Compute  $\tilde{Q} = \sum_{c=1}^C \omega_c \tilde{Q}_c$   

28:    Collect dataset  $\hat{D}$  by sampling feature vectors from  $\tilde{Q}$   

29:    for each rebalancing epoch  $e \in \{1, \dots, E_r\}$  do  

30:      Optimize  $W$  using equation 7  

31:    end for  

32:  end for

```

Algorithm 1 provides the pseudo-code for a generic task t in the HGP framework.